Sensors and Materials, Vol. 36, No. 1 (2024) 149–154
MYU Tokyo

S & M 3504

Comparison Between Neutron Bragg Dip and Electron Backscatter Diffraction Images of TlBr Semiconductors

Kenichi Watanabe,[1*] Yusuke Sugai,[1] Sota Hasegawa,[1] Keitaro Hitomi,[2] Mitsuhiro Nogami,[2] Takenao Shinohara,[3] Yuhua Su,[3] Joseph Don Parker,[4] and Winfried Kockelmann[5]

[1]Department of Applied Quantum Physics and Nuclear Engineering, Kyushu University, 744 Motooka, Nishi-ku, Fukuoka 819-0395, Japan
[2]Department of Quantum Science and Energy Engineering, Tohoku University, Aoba, Aramaki, Aoba-ku, Sendai 980-8579, Japan
[3]J-PARC Center, Japan Atomic Energy Agency, 2-4 Shirane, Shirakata, Tokai-Mura, Ibaraki 319-1184, Japan
[4]Neutron Science and Technology Center, Comprehensive Research Organization for Science and Society, 162-1 Shirakata, Tokai-Mura, Ibaraki 319-1106, Japan
[5]STFC, Rutherford Appleton Laboratory, ISIS Facility, Harwell, Oxford, OX11 0QX, United Kingdom

(Received September 23, 2023; accepted December 5, 2023)

Keywords: TlBr semiconductor detector, neutron diffraction, energy-resolved neutron imaging, electron backscatter diffraction

Thallium bromide (TlBr) semiconductor detectors are promising candidates for high-detection-efficiency, high-energy-resolution, and room-temperature gamma-ray spectrometers. In this study, we conducted neutron Bragg dip and electron backscatter diffraction (EBSD) imaging of TlBr crystals to measure the crystal orientation distribution. We confirmed that crystal grains were continuous over a certain distance along the solidification direction for samples fabricated with the current growth procedure. Finally, we compared the crystal orientation maps obtained with the two techniques. The two types of maps showed similar patterns. We concluded that EBSD, which can observe only surfaces, can be utilized to assess the uniformity of the bulky TlBr crystal, especially when observing the crystal surface perpendicular to the solidification direction.

1. Introduction

Thallium bromide (TlBr) semiconductor detectors are promising candidates as high-energy-resolution gamma-ray spectrometers.[1–10] Owing to the high effective atomic number (Tl = 81, Br = 35) and high density (7.56 g/cm^3) of TlBr, TlBr detectors are expected to have high detection efficiency. In addition, since the 2.68 eV bandgap energy of TlBr is relatively high, TlBr detectors can operate at room temperature. This is an important advantage over high-purity germanium semiconductor detectors. In the detector fabrication process, the crystal can be directly grown from the melt because of its congruent melting point of 460 °C and the absence of destructive phase transitions below its melting point. Owing to these promising physical

*Corresponding author: e-mail: k-watanabe@nucl.kyushu-u.ac.jp
https://doi.org/10.18494/SAM4629

ISSN 0914-4935

properties of TlBr, numerous researchers have pursued the development of gamma-ray detectors using TlBr.

Through improvements in the purification process of TlBr, its carrier transport characteristics have been improved.[11] As a result, the mobility–lifetime products of electrons and holes in TlBr have been improved. Consequently, TlBr semiconductor detectors show an excellent energy resolution of approximately 1% for 662 keV gamma rays.[4–10] However, these excellent performances were observed for relatively small detectors. To achieve high performance in large crystals, improved uniformity of the crystal quality is required. So far, we have demonstrated the evaluation of the 2D distribution of the crystal lattice orientation of TlBr using neutron Bragg dip imaging, which is a technique based on neutron diffraction.[12] This technique is useful for confirming the uniformity of the crystal quality, especially for bulky samples, such as gamma-ray detector materials, owing to the high penetration power of neutrons. However, it can only be performed at large pulsed neutron facilities, such as J-PARC in Japan and ISIS in the UK. To optimize the fabrication processes for large detectors, a more accessible crystal quality evaluation technique is desired. Electron backscatter diffraction (EBSD) can also be applied to evaluate the spatial distribution of the crystal orientation.[13] Although the usability of this technique is greater than that of neutron diffraction, only information on the sample surface can be obtained. To apply EBSD to evaluate a TlBr detector, we must reveal the conditions under which EBSD can be used to evaluate the quality of bulky crystal samples.

In this study, we compare neutron Bragg dip and EBSD images of TlBr crystals. In addition, we reveal the conditions under which EBSD can evaluate the uniformity of the bulky TlBr crystal. The crystal growth features are considered to be strongly related to the crystal growth processes of the TlBr.

2. Materials and Methods

2.1 Sample preparation

We prepared two types of TlBr single-crystal samples: the first was to confirm the crystal growth features of TlBr and the second was for comparison between neutron Bragg dip and EBSD imaging. Before the crystal growth process, the raw material was purified using a horizontal zone purification method.[11] The process was repeated more than 100 times. Then, a TlBr crystal was grown by the traveling molten zone method. To confirm the features of crystal growth, the grown TlBr crystal ingot was cut into a disk shape along the crystal solidification direction, as shown in Fig. 1. To obtain a sample for comparison between neutron Bragg dip and EBSD imaging, the crystal ingot was cut into a disk shape perpendicular to the ingot axis. This cutting procedure is generally used in the fabrication of TlBr detectors. The surfaces of the cut samples were polished for the EBSD analysis.

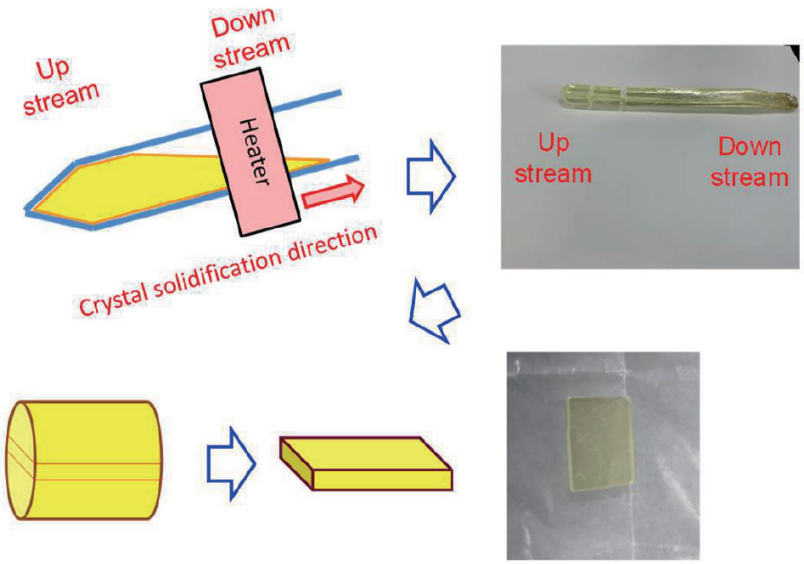

Fig. 1. (Color online) Sample preparation procedure for confirmation of the crystal growth features. The grown TlBr crystal ingot was cut into a disk shape along the crystal solidification direction.

2.2 Crystal orientation distribution measurements

We conducted neutron Bragg dip and EBSD imaging experiments to determine the TlBr crystal orientation distribution. Neutron Bragg dip imaging is a neutron diffraction technique based on energy-resolved neutron imaging. We acquired energy-resolved images of the two types of samples at RADEN beamline (BL-22) at the pulsed neutron facility J-PARC, Japan.[14] The neutron flux of the facility was more than 1×10^6 n/cm^2/s and depended on the selected collimator. By using a time-resolved neutron detector, we determined the neutron energy or wavelength using the time-of-flight technique. We applied the micro pixel chamber based neutron imaging detector using boron neutron converter (boron μ-NID) as a 2D neutron detector with time-resolved capability.[15] Figure 2 shows a photograph of the measured samples placed in front of the detector. The field of view of the boron μ-NID was 100×100 mm^2. By rearranging the time-resolved and 2D data, the neutron transmission spectra were obtained at all pixels. In this data processing, the pixel size was set to 400 mm. For a single crystal, the transmission spectrum shows a dip structure at the neutron wavelength, at which neutrons are diffracted out of the incident beam direction. Our knowledge of the TlBr crystal structure allowed us to prepare dip patterns for all crystal orientations. We determined the crystal orientation by pattern matching to the measured dip pattern.[12]

The EBSD measurements were conducted using a scanning electron microscope (Zeiss, ULTRA55) at the Ultramicroscopy Research Center, Kyushu University. The step size of the EBSD measurements was 40 m. A crystal orientation map was created by analyzing the diffracted electron pattern.[13]

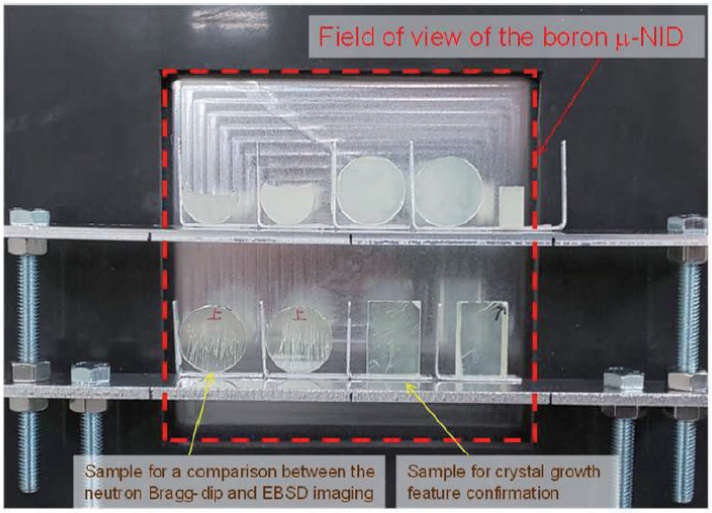

Fig. 2. (Color online) Photograph of the samples placed for neutron Bragg dip imaging. The field of view of the boron μ-NID was 100 × 100 mm^2.

3. Results and Discussion

Figure 3(a) shows the neutron Bragg dip image of the TlBr disk sample for confirmation of the crystal growth features. This figure shows an inverse pole figure map. The EBSD image is also shown in Fig. 3(b) for comparison. From these figures, we can confirm that crystal grains grow along the crystal solidification direction. This means that the crystal orientation of bulky grains can be seen on the surface of a disk wafer sample cut perpendicular to the solidification direction or the ingot axis.

To verify the above speculation, we observed the sample cut perpendicular to the ingot axis. Figure 4 shows the neutron Bragg dip and EBSD images of the TlBr disk sample to enable comparison between the two methods. The EBSD image is in good agreement with the one obtained with the neutron Bragg dip technique. The two images have similar patterns. Note that there are some differences between them. This is because the neutron Bragg dip image shows the predominant crystal orientation along the neutron path, while EBSD only provides information from the surface. However, in the TlBr crystal fabricated with the current growth procedure, crystal grains were continuous over a certain distance along the solidification direction. Therefore, we conclude that EBSD can be utilized to assess the uniformity of a bulky TlBr crystal, especially when observing the crystal surface perpendicular to the solidification direction. EBSD can be more easily conducted than neutron Bragg dip imaging, making it valuable for optimizing the growth conditions of TlBr crystals.

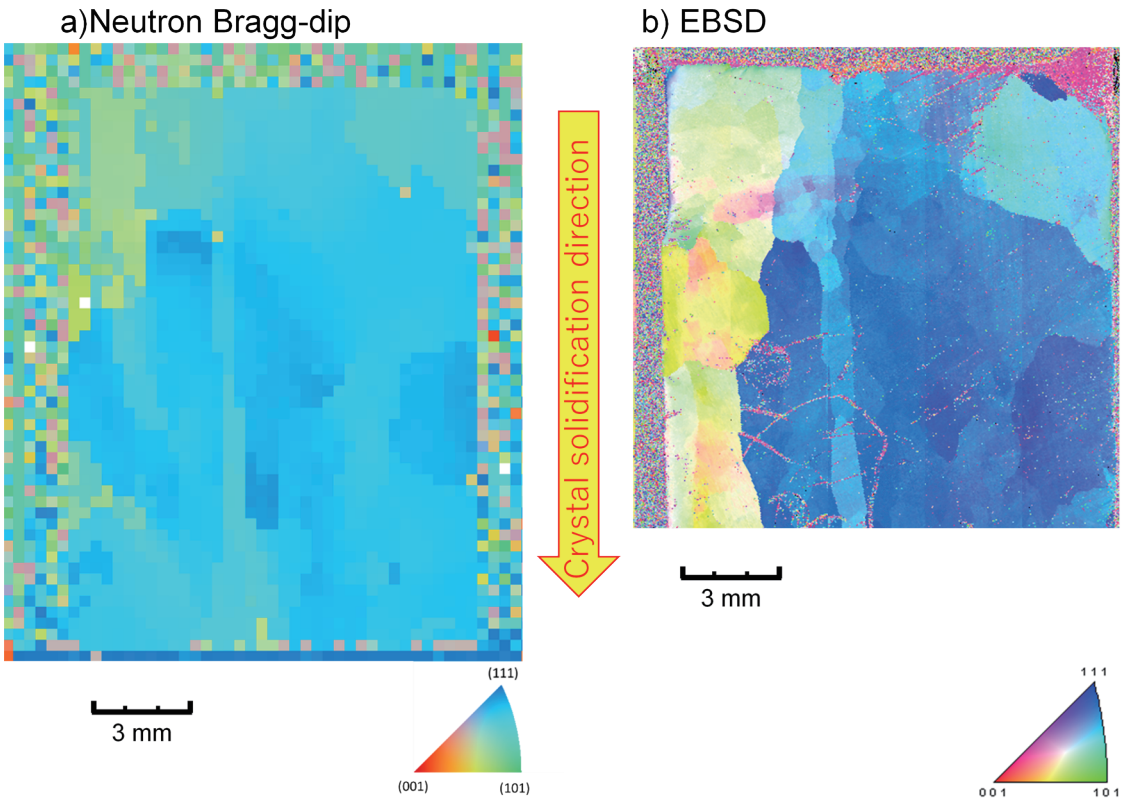

Fig. 3. (Color online) (a) Neutron Bragg dip and (b) EBSD images of the TlBr disk sample for confirmation of the crystal growth features.

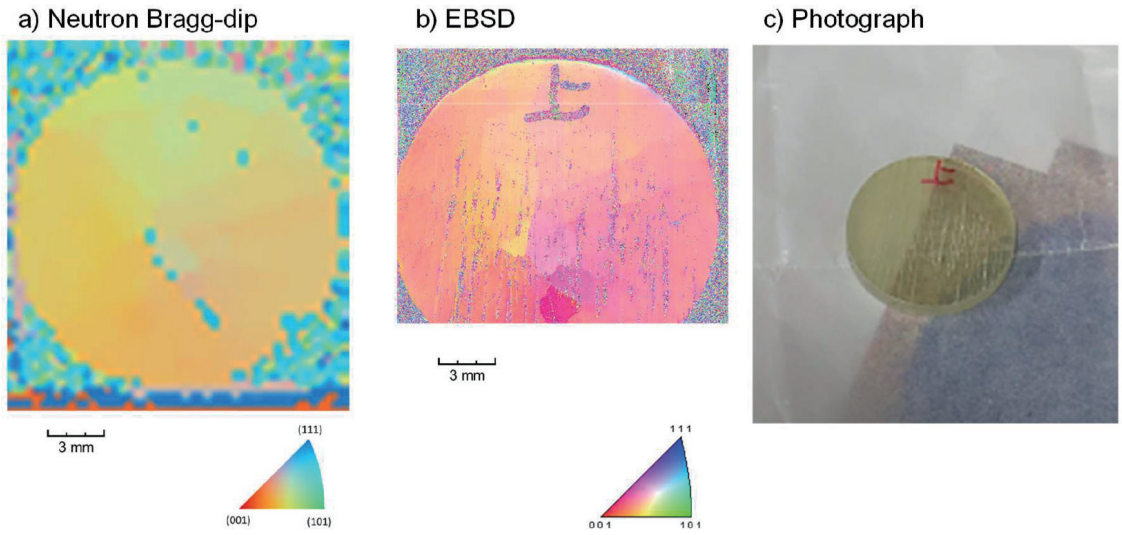

Fig. 4. (Color online) (a) Neutron Bragg dip and (b) EBSD images and (c) photograph of the TlBr disk sample for comparison between the two imaging techniques.

4. Conclusions

We conducted neutron Bragg dip and EBSD imaging of TlBr crystals to measure the crystal orientation distribution. To confirm the crystal growth features, we observed a sample cut into a disk shape perpendicular to the crystal solidification direction. We confirmed that crystal grains were continuous over a certain distance along the solidification direction for the samples fabricated with the current growth procedure. Additionally, we compared the crystal orientation maps obtained with the two techniques for the sample cut into a disk shape perpendicular to the solidification direction. The two types of images showed similar patterns. The neutron Bragg dip image shows the predominant crystal orientation to be along the neutron path, while EBSD provides information only from the surface. However, we can conclude that EBSD can be utilized to assess the uniformity of a bulky TlBr crystal, especially when observing the crystal surface perpendicular to the solidification direction.

As future work, we will reveal the relationship between the crystal quality and the carrier transport performance. On the basis of such knowledge, we will optimize the fabrication process of TlBr detectors to realize large and high-performance detectors.

Acknowledgments

This work was partially supported by JSPS KAKENHI Grant Number JP 22H02008. This study was also partially supported by a collaboration with Chubu Electric Power Company Inc. and the Cooperative Research Project of Research Institute of Electronics, Shizuoka University. The neutron experiment at the Materials and Life Science Experimental Facility of J-PARC was performed under a user program (Proposal No. 2021B0024).

References

1 K. Hitomi, T. Murayama, T. Shoji, T. Suehiro, and Y. Hiratate: Nucl. Instrum. Methods Phys. Res. A **428** (1999) 372.
2 K. Hitomi, O. Muroi, T. Shoji, T. Suehiro, and Y. Hiratate: Nucl. Instrum. Methods Phys. Res. A **436** (1999) 160.
3 T. Onodera, K. Hitomi, T. Shoji, and Y. Hiratate: Nucl. Instrum. Methods Phys. Res. A **525** (2004) 199.
4 K. Hitomi, T. Onodera, T. Shoji, and Z. He: Nucl. Instrum. Methods Phys. Res. A **578** (2007) 235.
5 K. Hitomi, T. Shoji, and Y. Niizeki: Nucl. Instrum. Methods Phys. Res. A **585** (2008) 102.
6 K. Hitomi, Y. Kikuchi, T. Shoji, and K. Ishii: Nucl. Instrum. Methods Phys. Res. A **607** (2009) 112.
7 B. Donmez, Z. He, H. Kim, L. J. Cirignano, and K. S. Shah: Nucl. Instrum. Methods Phys. Res. A **623** (2010) 1024.
8 K. Hitomi, T. Shoji, and K. Ishii: J Cryst. Growth **379** (2013) 93.
9 K. Hitomi, T. Tada, T. Onodera, S.-Y. Kim, Y. Xu, T. Shoji, and K. Ishii: IEEE Trans. Nucl. Sci. **60** (2013) 1156.
10 K. Hitomi, T. Onodera, S-Y. Kim, T. Shoji, and K. Ishii: Nucl. Instrum. Methods Phys. Res. A **747** (2014) 7.
11 K. Hitomi, T. Onodera, and T. Shoji: Nucl. Instrum. Methods Phys. Res. A **579** (2007) 153.
12 K. Watanabe, K. Matsumoto, A. Uritani, K. Hitomi, M. Nogami, and W. Kockelmann: Sens. Mater. **32** (2020) 1435.
13 B. L. Adamus, S. I. Wright, and K. Kunze: Metall. Trans. A **24** (1993) 819.
14 T. Shinohara, T. Kai, K. Oikawa, T. Nakatani, M. Segawa, K. Hiroi, Y. Su, M. Ooi, M. Harada, H. Iikura, H. Hayashida, J. D. Parker, Y. Matsumoto, T. Kamiyama, H. Sato, and Y. Kiyanagi: Rev. Sci. Instrum. **91** (2020) 043302.
15 J. D. Parker, M. Harada, H. Hayashida, K. Hiroi, T. Kai, Y. Matsumoto, T. Nakatani, K. Oikawa, M. Segawa, T. Shinohara, Y. Su, A. Takada, T. Takemura, T. Taniguchi, T. Tanimori, and Y. Kiyanagi: Proc. Int. Conf. Neutron Optics, JPS Conf. Proc. **22** (2018) 011022.